



Semnan University



## Delamination Analysis in Composite Root of a Carbon-Layer Reinforced Wind Turbine Blade

M.H. Safari Naderi <sup>a</sup>, H. Ekhteraei Toussi <sup>b</sup>, A. Ghasemi Ghalebahman <sup>a\*</sup>

<sup>a</sup> Mechanical Engineering Department, Semnan University, Semnan, Iran

<sup>b</sup> Mechanical Engineering Department, Ferdowsi University of Mashhad, Mashhad, Iran

### PAPER INFO

#### Paper history:

Received 2018-12-18

Received in revised form  
2019-02-15

Accepted 2019-04-26

#### Keywords:

Delamination  
Laminated composites  
Abaqus analysis  
Three-point bending test  
Cohesive zone model

### ABSTRACT

The inconsistencies accompanied with material properties typically cause the rise of delamination risk in composites made of different types of glass and carbon fibers. In this study, the delamination of a composite beam reinforced with a carbon layer under bending load is investigated. To this end, a small piece of a wind turbine blade root in the form of a heterogeneous laminated plate is simulated and analyzed. The methodology consists of two parallel approaches, including the experimental measurements and computer simulations. In the experimental program, the delamination of different specimens has been examined by three-point bending (3PB) tests. The diagrams of load versus load line displacement are recorded. In computer simulation, the geometry of composite laminate is re-modeled and stress analysis is performed. The results confirm that delamination loads obtained from the simulations are reliable and in good agreement with those obtained from the experimental procedures. The results of experimental measurements and computational simulations are utilized to predict the delamination failure and to optimize the lay-up sequence of the reinforced structure.

© 2019 Published by Semnan University Press. All rights reserved.

## 1. Introduction

In recent years, the use of composite materials in various industrial applications such as aerospace and automotive industries have been increased considerably. A composite structure is a material consists of two or more parts in the form of matrix, filler and reinforcement. In other words, composites are macroscopic combinations of two or more distinctive materials bounded effectively [1]. The strengthening part which is called reinforcement, usually increases the strength and prevents the initiation and propagation of cracks. Such part may be made of thin fibers with high resistance or granular particles. If they are mechanically well attached to the matrix, the reinforcement can greatly improve the properties of the composite material.

As in this kind of material, the ratio of strength to weight is higher than other types of engineering materials, the application of these materials have grown appreciably. Other important factors such as toughness, shock and vibration absorption, high fatigue life, high corrosion resistance and chemical agents have also been addressed by different researchers [2].

One main group of composite materials are laminated composites which are developed by combining several isotropic or anisotropic thin polymer sheets together. Increasing the use of such composite materials requires the study and understanding of their failure modes and the development of the technologies necessary to continuously improve their performance. In layered composites, the main mode of failure is called interlaminar fracture or delamination. The onset of

\* Corresponding author. Tel.: +98-23-31533349  
E-mail address: [ghasemi@semnan.ac.ir](mailto:ghasemi@semnan.ac.ir)

delamination is often induced inside the composite material and hidden from eye-inspection. The delamination damage may grow under different conditions of loading and significantly reduce the strength and life expectancy of the structure. The interlaminar crack growth is often associated with other destructive modes, especially the matrix cracking [3].

Recently, delamination analysis of composite laminates has been widely studied. Increasing the use of composite materials in various applications encourages researchers to make more detailed studies on the onset and growth of this phenomenon. This issue could be evaluated in analytical, numerical and empirical methods. Based on previous records, three basic modes of failure may be expected; these include the first or opening mode, the second or in-plane shearing (sliding) mode, and the third or anti-plane shearing (tearing) mode.

The onset of delamination growth in laminates may be influenced by geometrical parameters, mechanical properties of fibers and resin, and other factors such as number, lay-up and thickness of layers. An approach to simulate the propagation of delamination is the finite element method which is based on the local stress analysis around the tip of delaminated crack. In this method, the propagation occurs when a combination of energy release rate components at the tip of the crack, i.e.  $G_I$ ,  $G_{II}$  and  $G_{III}$ , is increased up to a specific value called the fracture toughness ( $G_c$ ). In fact, this value can be regarded as the material resistance against the crack growth, representing the material ability prior to fracture. However, in laminated composites, the separation of layers usually occurs in the interfacial surfaces. The main part of the unknowns in fracture analysis is the detection of damage position which may be clear to a designer using non-destructive evaluations. This means that the location and path of damage initiation may be regarded as some defined parameters before performing a fracture analysis. Accordingly, there is a simple and yet a precise methodology to apply, the so-called cohesive zone model (CZM). The method of CZM is based on dictating a degree of tendency for separation of risky layers in contrasting its ability to connect the layers in terms of a traction-separation rule [4].

For the first time, Nydelman [5] utilized the polynomial functions for the adhesion rule and used this model to characterize the creation of holes. Tvergaard [6] presented a trapezoidal model for calculating the resistance to crack growth in elasto-plastic materials. Suresh [7] used a linear adhesion rule to investigate the intergranular failure

behavior. In his model, intermediate tension increases linearly with the opening of the interfacial boundary to reach a critical value. Afterwards, it decreases and eventually reaches zero. Camacho and Erythes [8], using a sticky linear reduction model, investigated the expansion of several cracks in brittle materials under impact loading. Camano et al. [9] performed a composite structure failure using the CZM. The results of this study indicated that the method of CZM is efficient in modeling of delamination phenomenon.

Accordingly, using the CZM within the Abaqus finite element framework, the growth of interlayer cracks in the root of a wind turbine blade is modeled.

Relying on verified Abaqus simulations, the delamination of carbon reinforced laminate and the extraction of the proper position for the carbon reinforced layer across the thickness of a composite beam are the main purposes of the present paper.

## 2. Damage Initiation Criteria for the Adhesive Zone

There are different formulations to connect interlaminar traction level and maximum strain or debonding stretch into delamination of composite laminates, some of which are introduced in this section. One of the well-known correlations is known as the uncoupled constitutive relation of cohesive conjunction which is provided in the following [10]:

$$\mathbf{t} = \begin{Bmatrix} t_n \\ t_s \\ t_t \end{Bmatrix} = \begin{bmatrix} k_{nn} & 0 & 0 \\ 0 & k_{ss} & 0 \\ 0 & 0 & k_{tt} \end{bmatrix} \begin{Bmatrix} \epsilon_n \\ \epsilon_s \\ \epsilon_t \end{Bmatrix} = \mathbf{K} \boldsymbol{\epsilon} \quad (1)$$

where the vector  $\mathbf{t}$  is the nominal stress vector with a component  $t_n$  in normal-to-interface direction as well as the other two components  $t_s$  and  $t_t$  in shearing directions. Also, the matrix  $\mathbf{K}$  is the elastic or constitutive matrix and vector  $\boldsymbol{\epsilon}$  collected the strain tensor elements and its components are calculated as follows:

$$\epsilon_n = \frac{\delta_n}{T_o}, \epsilon_s = \frac{\delta_s}{T_o}, \epsilon_t = \frac{\delta_t}{T_o} \quad (2)$$

In this case,  $\delta_n$ ,  $\delta_s$  and  $\delta_t$  are the amounts of maximum stretch at the onset of delamination in one normal and two shearing directions respectively, and  $T_o$  is the thickness of the adhesive layer.

In order to predict the instant of delamination correctly, there are four criteria, including two criteria based on elasticity and two criteria in terms of strains [10]. In general, a combined mode of loading would be considered. Here, the parameters  $t_n^o$ ,  $t_s^o$  and  $t_t^o$  are maximum values of nominal stress (mode

I) or shearing stresses (modes II & III). Moreover,  $\epsilon_n^o$ ,  $\epsilon_s^o$  and  $\epsilon_t^o$  are denoted as the corresponding nominal strains in the aforementioned states. In general, the criteria for damage initiation can be divided into four categories. The first criterion is the maximum nominal stress. In this criterion, the damage begins when the stress in the elements adjacent to the interface has reached a maximum level. This criterion can be stated by using the following equation:

$$\text{Max} \left\{ \frac{t_n}{t_n^o}, \frac{t_s}{t_s^o}, \frac{t_t}{t_t^o} \right\} = 1 \tag{3}$$

In the maximum nominal strain criterion, the damage initiation is predicted using the strain values of intermediate element. When the maximum value of the normalized strain components reaches 1, the damage begins. That is:

$$\text{Max} \left\{ \frac{\epsilon_n}{\epsilon_n^o}, \frac{\epsilon_s}{\epsilon_s^o}, \frac{\epsilon_t}{\epsilon_t^o} \right\} = 1 \tag{4}$$

The third one is the second-order nominal stress criterion in which the interconnections between stresses in different modes are coupled together through a quadratic relationship. In this criterion, the damage will occur when the following relationship is established:

$$\left\{ \frac{t_n}{t_n^o} \right\}^2 + \left\{ \frac{t_s}{t_s^o} \right\}^2 + \left\{ \frac{t_t}{t_t^o} \right\}^2 = 1 \tag{5}$$

Eventually, in the second-order nominal strain criterion, the interaction of strains is modeled using the following relationship for the strain levels [11]:

$$\left\{ \frac{\epsilon_n}{\epsilon_n^o} \right\}^2 + \left\{ \frac{\epsilon_s}{\epsilon_s^o} \right\}^2 + \left\{ \frac{\epsilon_t}{\epsilon_t^o} \right\}^2 = 1 \tag{6}$$

In this research, the quadratic nominal stress criterion for the prediction of interlayer separations have been used.

### 3. Finite Element Modelling

This study is based on the efficient application of a verified computer code to predict the commencement of damages in the laminated composite media. So, at the beginning, a proper modelling phase must be done. Accordingly, in this study about 10000 elements of SC8R-type are used

for the simulations. Prior to the analysis, a complete mesh sensitivity test has been done to guarantee the convergence of the solution. Then the solution domain is discretized and the analysis has been performed. The details of the analysis are explained in the following section.

#### 3.1. Sample specifications, boundary conditions and loading

In order to conduct the experimental investigation, 36 standard test samples were prepared for the evaluations. The experimental measurements include initial tests for the determination of adhesion bonding parameters of the glass and carbon layers as well as the main tests devoted to three-point bending (3PB) setups. In calibration phase, sample specimens are placed under simple uniaxial tensile and shear loading conditions. In this case, the results of the experimental tests are used to find  $k_{nn}$ ,  $k_{ss}$  and  $k_{tt}$  strength parameters appeared in Eq. (1). Afterwards, by plotting the force versus load line displacement, for different beam installations, the strength of composite beam in different configurations are found. In this stage, six samples are placed under 3PB-loading conditions. Amongst them, three samples have 47 glass-epoxy layers, two specimens contain 22 glass-epoxy and carbon-epoxy layers, and one specimen contains 69 glass-epoxy and carbon-epoxy layers similar to those provided in the root of wind turbine blade. The elastic properties and lay-up stacking sequences of glass-epoxy layers with [0,90] and [45,-45] configurations and also those for unidirectional carbon-epoxy and glass-epoxy layers are empirically measured based on ASTM D3039 standard and consequently, their results are shown in Tables 1 and 2. The stiffness coefficient of single laminates along the fiber direction is designated by  $E_1$ , in transversal direction by  $E_2$  and in thickness direction by  $E_3$ . Besides, according to experimental results, the deviation of different orthotropic shear modulus and Poisson's ratio components are negligible. Therefore, such parameters are simply represented by unique  $G$  and  $\nu$  symbols, respectively.

**Table 1.** Elastic properties of single lamina.

	$E_1$ (N/mm <sup>2</sup> )	$E_2$ (N/mm <sup>2</sup> )	$E_3$ (N/mm <sup>2</sup> )	$\nu_{12}=\nu_{13}=\nu_{23}$	$G_{12}=G_{13}=G_{23}$ (N/mm <sup>2</sup> )
Epoxy-glass [0/90]	20000	16500	2000	0.3	4000
Epoxy-glass [45/-45]	19000	19000	2000	0.3	2300
Unidirectional epoxy-glass	30000	3000	2000	0.3	4000
Unidirectional epoxy-carbon	80000	6000	2000	0.3	5700

**Table 2.** Layer stacking sequences considered in the root of wind turbine blade.

Row	Material	Number of Layers
1	Glass-Epoxy [45/-45]	5
2	Unidirectional glass-epoxy	12
3	Glass-Epoxy [45/-45]	5
4	Glass-Epoxy [0/90]	3
5	Glass-Epoxy [45/-45]	2
6	Glass-Epoxy [0/90]	2
7	Glass-Epoxy [45/-45]	7
8	Glass-Epoxy [0/90]	13
9	Glass-Epoxy [45/-45]	5
10	Unidirectional glass-epoxy	7
11	Unidirectional carbon-epoxy	2
12	Glass-Epoxy [45/-45]	1
13	Glass-Epoxy [0/90]	2
14	Glass-Epoxy [45/-45]	3

The dimensions of the 3PB specimens are shown in Table 3. It is worth noting that the composite beam samples with 30, 50, 70, 90 and 200 mm length, and 27 and 47 number of layers are fabricated similar to those used in the turbine blade root.

In the modeling phase, firstly, the layers are configured according to the specified material lay-up. The region filled with the resin has been simulated by an interlayer continuous shell element. In this step, the epoxy mechanical properties are considered for the interlayer material. These properties are measured directly according to ASTM D2095 and ASTM D5868 standards and their obtained results are presented in Table 4.

The bounding parameters introduced in Eq. (1) are used to assess the risk of delamination failure. In this manner, once the coupling of two successive glass-epoxy layers are mattered, the properties of glass-epoxy-glass bonding are used, and when the two layers are made of carbon-epoxy, the carbon-epoxy-carbon bonding properties are used. In this analysis, it is assumed that the specimens are placed under 3PB displacement control conditions with 4mm mid-span displacement.

### 3.2. Results of finite element analysis

Usually the finite element softwares used in mechanical engineering are based on a numerical technique for modeling a complex structure. The basic concept of finite element method is that the field distribution of each continuous variable, such as velocity, stress, pressure, or temperature, can be approximated by a discretized model which includes a set of continuous field variables, which are separated in piecewise subsets or elements. In this case, the variables are defined in limited number of subsets.

**Table 3.** Dimensions of 3PB test specimens.

Row	Supports distance (mm)	Length (mm)	Width (mm)	Height (mm)
1	30	141	24.75	11.6
2	50	141	22.4	11.6
3	70	129	34.5	5.7
4	90	142.6	23.27	11.6
5	200	300	70	17

**Table 4.** Adhesion properties of epoxy resin.

Test	$k_n$ (MPa)	$k_s$ (MPa)	$k_t$ (MPa)
Glass-epoxy-glass bond	6.006	2.31	2.31
Carbon-epoxy-carbon bond	4.74	1.82	1.82
Glass-epoxy-carbon bond	4.89	1.88	1.88

Among the many software platforms operated on the category of finite element-based techniques, one of the most authoritative and powerful software tools that engineers and researchers utilize is the renowned software of Abaqus. Modeling in Abaqus starts with shape modeling and definition of properties of samples. In the modeling carried out here, the geometric structures of composite layers are modeled in the form of continuum shell elements.

In order to model a multi-layered composite with continuous shell elements, only one element is used in the thickness direction for each layer. In other words, a multilayered shell is synthesized by a combination of several shell elements. In continuous elements, the lay-up sequence of the layers must be considered.

With regard to simulation of composite beams examined in this paper, during the preliminary studies performed, a considerable difference has been observed between shell and continuum shell elements. Due to the accuracy of shell elements in contact analysis, these elements have been used in simulations. The element used is an eight-node cubic type element. Accordingly, 3PB specimens with dimensions and lay-ups shown in Table 6 are modeled by two methods comprising the perfect connection method (i.e., contact between the successive layers considering the strength of the resin) and the CZM. After that, the destructive delamination phenomenon is simulated according to the traction-separation rules.

In order to recognize the beginning of delamination process in 3PB tests, a proper criterion is needed. There are four accessible criteria for the assessment of these failures [11] introduced in Eqs. (3-6). For the present work analysis in each comparison

study, Eqs. (3) and (5) are utilized. As a whole, it is found that the results obtained from quadratic stress criterion in (5) are closer to the results of experiments.

In simulation phase, the effect of support distance on response of 3PB testing has been examined. To this end, three samples with lay-ups similar to the first 47 layers of the blade root with support spans of  $U=30, 50$  and  $90$  mm are considered for the analyses. Assuming elastic properties for the material, the simulation results are supposed to be linear. Fig. 1 represents the mesh pattern used in finite element solutions of Abaqus.

Fig. 2 illustrates the results of such simulations in which the curves are protracted until the criterion of damage initiation is carried out.

One specimen is made of the 22 lower-most layers of the turbine blade root in which carbon layer is located downward near the beam support. Another specimen is made of reverse delamination sequence in which carbon layer is placed upward. The aforementioned specimens are simulated under 3PB test conditions with  $70$  mm support spacing distance. The results of these simulations are presented in Fig. 3 and the results are protracted up to the damage initiation limit.

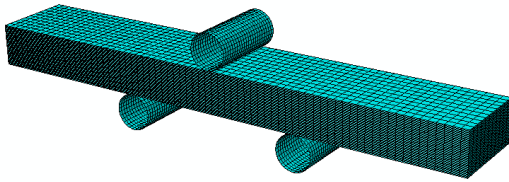


Fig. 1. The finite element model.

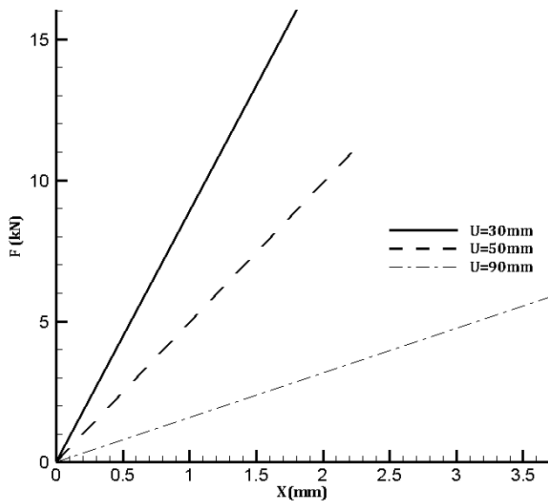


Fig. 2. The 3PB load-displacement obtained by simulation of three 47-layer laminates with different supports spans.

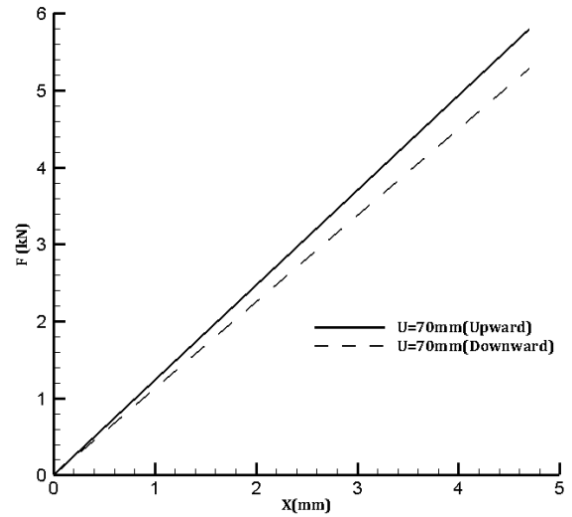


Fig. 3. The 3PB load-displacement simulation of 22-ply laminate with  $70$  mm supports distance.

As the results of finite element analysis are continued until the onset of damaging, the force-displacement results are also recorded until the satisfaction of damage criterion. Moreover, another sample made of 69 layers fulfilling the conditions at the root of the turbine blade is simulated. This specimen is located on the roller supports  $200$  mm apart and tested under 3PB conditions. The results of this simulation before the onset of damage initiation are also presented in Fig. 4.

In the following, comparing the results of simulation and experimental tests, a method is introduced to predict the delamination onset in composite sheets reinforced with carbon layers.

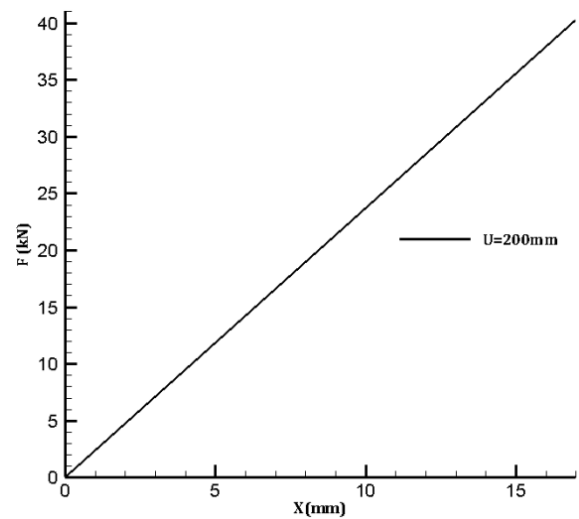


Fig. 4. The 3PB load-displacement diagram obtained by simulation of a 69-layer laminate with  $200$  mm supports distance.

### 3. Results of Experimental Tests

In order to study the delamination phenomenon by experimental and simulation approaches, the facilities of the material testing laboratory in Ferdowsi University of Mashhad have been used and 3PB tests have been performed on the prepared composite specimens. To this end, six samples have been fabricated similar to the layered part of the wind turbine blade roots by means of vacuum bagging technique. Among the six specimens, three samples have 47 glass-epoxy layers similar to the first 47 layers in turbine blade root, another sample made of 22 layers of glass-epoxy and carbon-epoxy is similar to the next 22 layers of the wind turbine blade and a sample is made similar to the full 69 layers of wind turbine blade root. In Fig. 5, the 3PB test specimen used for the study of delamination phenomenon is shown.

In the test stage, in addition to extracting and comparing the results of force and deformations, the fracture load level is assessed. In the 3PB test, the samples are loaded by upper plunger driven type under displacement control conditions. During the loading process, the force-displacement diagrams are recorded by a computer connected to the flexure testing machine.

To assess the delamination process during the test period, damaged area is examined by visual inspection and by photographic records. As stated before, using the extracted data, the force-displacement graphs are obtained. In these diagrams, the ordinate represents the force values in kN and the abscissa indicates the values of load-line displacements in mm. It is worth noting that, in order to increase the accuracy of the measurements, three samples are tested to control the repeatability. Also, in all samples, the loading is performed and measured at the same levels of the strain rate. In order to measure the delamination phenomenon in layered composites, three samples of 47-ply beam is examined. In Fig. 6, the experimental results for these three examples are depicted.

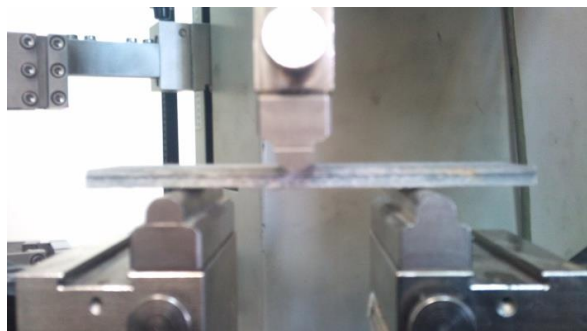


Fig. 5. A typical 3PB test setup.

As shown in Fig. 6, when the distance between the supports decreases, the delamination phenomenon occurs with smaller deformation and higher force levels. In Fig. 7, the inner layering of a typical beam can be seen.

At the next step, a 22-ply composite beam is placed over the roller supports of the flexural testing machine with 70mm apart and tested under 3PB conditions. The experimental results regarding the flexural testing are illustrated in Fig. 8.

Furthermore, another 22-layer specimen with reversed stacking sequence (in which carbon layer is located upward) is tested under 3PB conditions with a support distance of 70 mm. Accordingly, the load-displacement curve is extracted from the results of this experimental measurement and is depicted in Fig. 9.

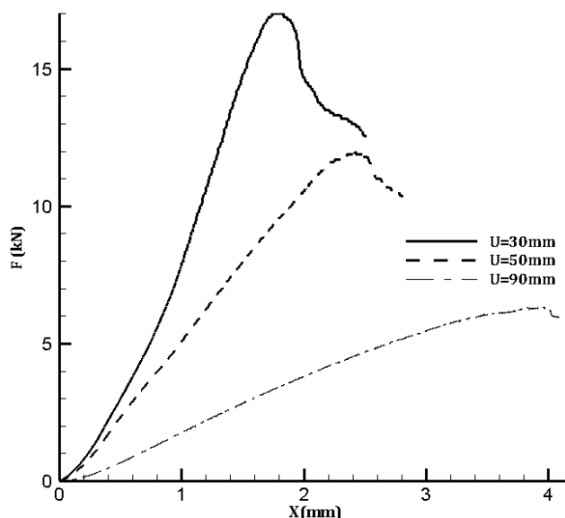
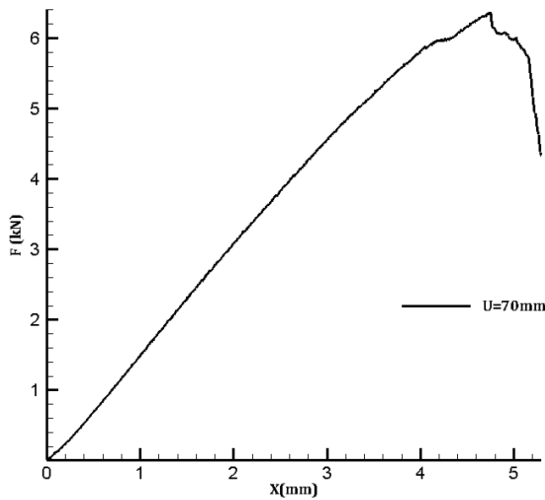
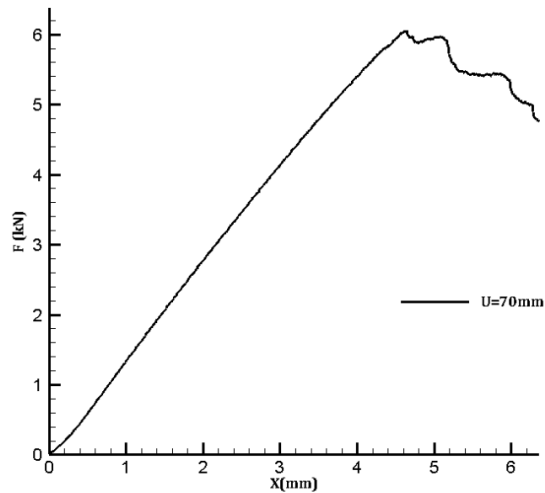


Fig. 6. The 3PB load-displacement diagrams obtained by experimental testing for the three 47-layer laminates with different supports spans.

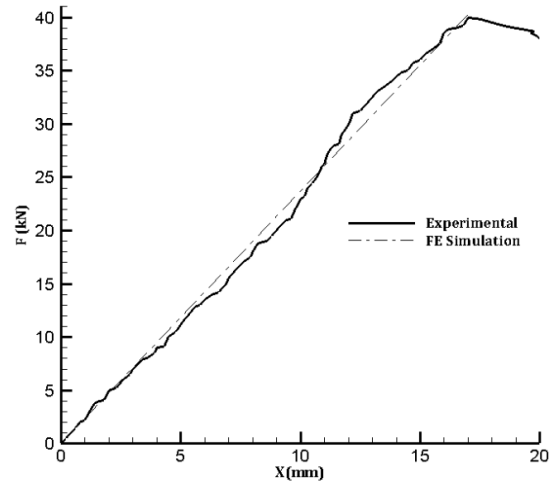


**Fig. 7.** The Delamination occurrence in 3PB test specimens.**Fig. 8.** The 3PB load-displacement curve obtained by experimental test on a 22-layer laminate with 70 mm supports width.**Fig. 9.** The 3PB load-displacement diagram obtained by experimental testing for a 22-layer laminate with 70 mm supports distance.

As it can be seen, when the carbon layer is located in the upper half of the beam cross section, the delamination phenomenon occurs in comparatively lower force and accordingly at a lower displacement level.

Besides, the 69-layer sample is located at a 200 mm support distance and tested in 3PB conditions. The corresponding load-displacement curve obtained from the results of this experimental measurement is shown in Fig. 10.

Due to the small slip that the sample have experienced during the test, the graph in the early stages is accompanied with irregular behaviors, which reduces in the next loading levels.

**Fig. 10.** The 3PB load-displacement curve obtained by experimental test for a 69-layer laminate with 200 mm supports distance.

Preventing the damage in composite structures is one of the most important issues for the engineers. There are two main types of damage mechanisms in the layered composites which may be integrated together in a complex way. These damage modes generally include the intra-layer failure and inter-layer delamination. The first type, which can be regarded as micro-mechanical failure, includes the fiber breakage, cracks emanation in the matrix and fiber-matrix debonding. The inter-layer damages which include the delamination problems, are the most important types of composite failure reasons. The likelihood of the occurrence for each of these two mechanisms usually restricts the design strategies [12]. In this research, in order to investigate and predict the delamination phenomenon, experimental measurements and computer simulations performed in Abaqus are carried out. For this purpose, several laminated composite beams with different stacking patterns are tested and simulated. The studied case includes the 47-layer beam models, fabricated similar to the first 47 layers of the wind turbine blade and a single 22-layer beam constructed similar to the lower-most part of the blade and also a complete 69-layer beam, similar to entire turbine wind blade root stacking pattern.

After collecting initial information and defining a suitable failure criterion, the method of CZM which relies on traction-separation rules has been utilized. Subsequently, quasi-static delamination analyses are performed for the 3PB test samples.

In order to study the delamination phenomenon in a layered composite, the calibrated strength data of epoxy adhesive is used in defining inter-layer contact properties. Besides, to benefit a higher level of accuracy in simulation stage, continuum shell

elements for the Abaqus modeling have been used. The results of simulation of 3PB test samples are compared with experimental results. Based on obtained results, the developed model is capable to predict the crack initiation region and the critical load of delamination with acceptable accuracy. In order to assess the precision of obtained results in identifying the delamination phenomenon, a comparison between the simulation and experimental results are made and presented in Table 5. The amounts of error percentages are also presented in this table. It is seen that CZM method which benefits the traction-separation rules and utilizes the continuum shell elements can be employed to study the propagation phenomenon in computer simulations and consequently obtain the comparable results.

Abaqus simulations are used to investigate and predict the onset of delamination phenomenon in layered composites. In this regard, one can predict the optimum position of carbon reinforced layer with acceptable level of accuracy. Due to the high elastic modulus of carbon-fiber reinforced laminates comparing the glass-fiber reinforced laminates, the strength of layered composites in which a carbon layer is used, can be enhanced appreciably. If the optimal position of carbon fiber layer is found, the highest level of beam strength could be achieved. For this purpose, the simulations of beams with different positions of carbon layers are performed under 3PB test. The results of this optimization are plotted in Fig. 10. In this figure, the ordinate shows the amount of applied force and the abscissa denotes the position of the carbon fiber layer ( $x$  is the distance between carbon layer and the upper surface of the beam and  $h$  is total thickness of the beam).

The curve shown in Fig. 11 can be approximated to obtain the following correlation in which  $\xi = x/h$ .

$$F = 29.44\xi^4 - 61.35\xi^3 + 50.68\xi^2 - 18.34\xi + 7.6 \quad (7)$$

With reference to Fig. 11, the center of the curve

is shifted towards the upper surfaces. It means that, once the carbon layer is located at the lower most position or underneath the beam, it can withstand the highest level of external loads. While locating the carbon reinforced layer in the vicinity of load application site (adjacent to the loading pin) would reduce the load capacity of the structure. This analysis reveals that carbon layer position affects the beam strength non-symmetrically and also it shows that locating the carbon layer in the lowermost position can be regarded as the best condition.

#### 4. Conclusions

In this study, the delamination phenomenon in a wind turbine blade root was investigated through performing a set of experiments and numerical simulations. In the experimental setup, several laminated composite beams with different stacking sequences were examined. In the simulation procedure, to achieve accuracy in predicting the onset of delamination and optimum position of carbon reinforced layer compared to those obtained by experiments, the contact surface between successive layers was modeled based on the CZM method with considering the properties of adhesion strength of the resin and using the application of the continuum shell elements.

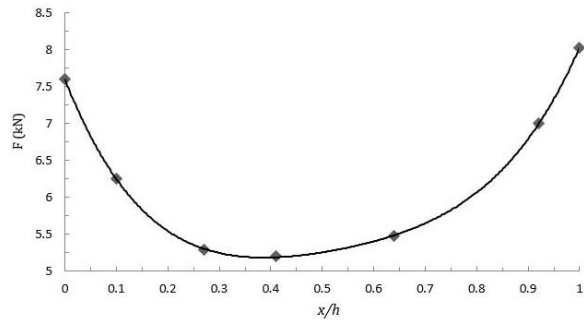


Fig. 11. Damaging force versus carbon layer position in 3PB test

Table 5. Experimental results and computer simulations of the 3PB test specimens

Test	Parameter	Experimental results	Simulation results	Error percent
3PB-test of 47-layer sample in 30 mm beam span	Force(N)	16990	16020	%5.7
	Displacement (mm)	1.8	1.8	
3PB-test of 47-layer sample in 50 mm beam span	Force(N)	11980.1	11390	%4.9
	Displacement (mm)	2.29	2.3	
3PB-test of 47-layer sample in 90 mm beam span	Force(N)	6337.8	5849	%7.7
	Displacement (mm)	3.7	3.75	
3PB-test of 22-layer sample in 70 mm beam span	Force(N)	6366	6073	%4.6
	Displacement (mm)	4.6	4.8	
3PB-test of 69-layer sample in 200 mm beam span	Force(N)	40000	40290	%0.7
	Displacement (mm)	16.9	17	

## References

- [1] Szekrenyes. Delamination of composite specimens. PhD Dissertation, Budapest University of Technology and Economics, Dept. Appl. Mechanics; 2005.
- [2] Ding W. Delamination analysis of composite laminates. PhD Dissertation, graduate Department of Chemical Engineering and Applied Chemistry, University of Toronto; 1999.
- [3] Villaverde NB. Variable mixed mode delamination in composite laminates under fatigue condition: testing and analysis, PhD dissertation, University of de Girona; 2004.
- [4] Jiang H. Cohesive zone model for carbon nanotube adhesive simulation and fracture/fatigue crack growth. PhD dissertation, University of Akron; 2010.
- [5] Xu XP, Nydelman A. Void Nucleation by Inclusion Debonding in a Crystal Matrix. *Modeling and Simulation in Materials Science and Engineering* 1993; 1: 111-132.
- [6] Tvergaard V, Hutchinson JW. The Relation between Crack Growth Resistance and Fracture Process Parameters in Elastic-Plastic Solids. *J. Mech. Phys. Solids* 1992; 40(6) 1377-97.
- [7] Ortiz M, Suresh S. Statistical Properties of Residual Stresses and Intergranular Fracture in Ceramic Materials. *J. Appl. Mech.* 1993; 60: 77-84.
- [8] Camacho G, Ortiz M. Computational Modeling of Impact Damage in Brittle Materials. *Int. J. Solids Struct.* 1996; 33: 2899-2938.
- [9] Comano PP, Davila CG, de Moura M. Numerical simulation of mixed mode progressive delamination in composite materials. *J. Comp. Mat.* 2003; 37: 1415-1438.
- [10] Benzeggagh ML, Kenane M. Measurement of Mixed-Mode Delamination Fracture Toughness of Unidirectional Glass/Epoxy Composites with Mixed-Mode Bending Apparatus. *Composites Science and Technology* 1996; 56: 439-449.
- [11] Camanho PP, Davila CG. Mixed-Mode Decohesion Finite Elements for the Simulation of Delamination in Composite Materials. *NASA/TM-2002-211737* 2002; 1-37.
- [12] Sorensen L, Botsis J, Gmur T, Humber L. Bridging tractions in mode I delamination: Measurements and simulations. *Comp. Sci. Technol.* 2008; 68: 2350-2358.

